Supplemental Material for "Diffusive Fizeau Drag in Spatiotemporal Thermal Metamaterials"

Liujun Xu[1,2], Guoqiang Xu[1], Jiping Huang[2*], and Cheng-Wei Qiu[1*]

[1]*Department of Electrical and Computer Engineering, National University of Singapore, Singapore 117583, Singapore*

[2]*Department of Physics, State Key Laboratory of Surface Physics, and Key Laboratory of Micro and Nano Photonic Structures (MOE), Fudan University, Shanghai 200438, China*

[*]email: jphuang@fudan.edu.cn; [*]email: chengwei.qiu@nus.edu.sg

Supplemental Note I: Proof of no direct thermal analog

Since the macroscopic heat does not carry any momentum, the biased advection carrying a momentum cannot generate a speed difference of temperature field propagation in two opposite directions, which is proved as follows.

Heat transfer in a two-dimensional homogeneous porous medium is governed by

$$\rho_0 \frac{\partial T}{\partial t} + \boldsymbol{\nabla} \cdot (\phi \rho_a \boldsymbol{u} T - \kappa_0 \boldsymbol{\nabla} T) = 0, \tag{S1}$$

with definitions of $\rho_0 = \phi\rho_a + (1-\phi)\rho_{s0}$ and $\kappa_0 = \phi\kappa_a + (1-\phi)\kappa_{s0}$. ρ_a (or ρ_{s0}) is the product of mass density and heat capacity of the fluid (or solid). κ_a (or κ_{s0}) is the thermal conductivity of the fluid (or solid). The substitution of a wavelike temperature field described by $T = \mathrm{e}^{\mathrm{i}(\beta x - \omega t)}$ into Eq. (S1) yields

$$-\mathrm{i}\omega\rho_0 + \mathrm{i}\beta\phi\rho_a u_x + \beta^2\kappa_0 = 0. \tag{S2}$$

Since we apply a periodic source with a temperature of $T(x=0) = \mathrm{e}^{-\mathrm{i}\omega t}$, ω is real and β is complex. We can take $\beta = p + \mathrm{i}q$, with p and q being two real numbers, so Eq. (S2) can be rewritten as

$$-\mathrm{i}\omega\rho_0 + \mathrm{i}(p+\mathrm{i}q)\phi\rho_a u_x + (p+\mathrm{i}q)^2\kappa_0 = 0, \tag{S3}$$

which can be further decomposed into two equations according to its real and imaginary parts,

$$-q\phi\rho_a u_x + (p^2 - q^2)\kappa_0 = 0, \tag{S4a}$$

$$-\omega\rho_0 + p\phi\rho_a u_x + 2pq\kappa_0 = 0. \tag{S4b}$$

The solutions to Eqs. (S4a) and (S4b) can be expressed as

$$p_{f,b} = \pm\frac{\sqrt{2}\gamma}{4\kappa_0}, \tag{S5a}$$

$$q_{f,b} = \frac{-8\phi\rho_a u_x \omega\rho_0\kappa_0 \pm \sqrt{2}\gamma\left(2\phi^2\rho_a^2 u_x^2 + \gamma^2\right)}{16\omega\rho_0\kappa_0^2}, \tag{S5b}$$

with a definition of $\gamma = \sqrt{-\phi^2\rho_a^2 u_x^2 + \sqrt{\phi^4\rho_a^4 u_x^4 + 16\omega^2\rho_0^2\kappa_0^2}}$. Since p_f and p_b are two

opposite numbers, the forward and backward speeds of temperature field propagation calculated by $|v_{f,b}| = |\omega/p_{f,b}|$ are the same. We further plot the thermal dispersion with different values of u_x in Fig. S1(a). $\omega(p_f) = \omega(p_b)$ always stands despite different values of u_x, indicating that there is exactly no speed difference of temperature field propagation in two opposite directions, i.e., no diffusive Fizeau drag.

We further confirm Eqs. (S5a) and (S5b) by finite-element simulations. As described by Eq. (S5b), the spatial decay rates in two opposite directions are different if $u_x \neq 0$. Therefore, when we set $u_x = 0$ mm/s, the forward and backward cases are the same [Fig. S1(b1)]. When we set $u_x = 5$ mm/s, the forward and backward cases are nonreciprocal, which is reflected in the different amplitudes of wavelike temperature fields. However, there is no time difference between the forward and backward cases. When we further set $u_x = 10$ mm/s, the nonreciprocity degree is enhanced [Fig. S1(b3)], manifesting as a larger amplitude difference of temperature fields. Again, no time difference appears. The analytical results described by Eqs. (S5a) and (S5b) are plotted with dotted curves, which are completely the same as the simulation results. Therefore, only the biased advection is unable to generate a speed difference, but it can contribute to an amplitude difference of temperature fields. In other words, it is highly nontrivial to reveal diffusive Fizeau drag in heat transfer due to the lack of macroscopic heat momentum to interact with the biased advection.

Supplemental Note II: Method of numerical calculations

To introduce spatial inhomogeneity to a porous medium, we keep the parameters of the fluid unchanged and modulate the parameters of the solid skeleton as

$$\rho_s(\xi) = \rho_{s0}\left(1 + \delta_\rho \cos(G\xi + \theta)\right), \tag{S6a}$$

$$\kappa_s(\xi) = \kappa_{s0}\big(1 + \delta_\kappa \cos(G\xi)\big), \tag{S6b}$$

where δ_ρ and δ_κ are the modulation amplitudes of the parameters of the solid skeleton with a definition of $\xi = x + \zeta y$. Therefore, the effective parameters of the inhomogeneous porous medium can be expressed as

$$\rho(\xi) = \phi\rho_a + (1-\phi)\rho_s(\xi) = \rho_0\left(1 + \Delta_\rho \cos(G\xi + \theta)\right), \tag{S7a}$$

$$\kappa(\xi) = \phi\kappa_a + (1-\phi)\kappa_s(\xi) = \kappa_0\big(1 + \Delta_\kappa \cos(G\xi)\big), \tag{S7b}$$

with definitions of $\Delta_\rho = (1-\phi)\delta_\rho\rho_{s0}/\rho_0$ and $\Delta_\kappa = (1-\phi)\delta_\kappa\kappa_{s0}/\kappa_0$. The governing equation of heat transfer in the inhomogeneous medium can be expressed as

$$\rho(\xi)\frac{\partial T}{\partial t} + \boldsymbol{\nabla}\cdot(\phi\rho_a \boldsymbol{u}T - \kappa(\xi)\boldsymbol{\nabla}T) = 0. \tag{S8}$$

We consider the upward advection with a speed of u_y, so Eq. (S8) can be expanded as

$$\rho(\xi)\frac{\partial T}{\partial t} + \phi\rho_a u_y\frac{\partial T}{\partial y} + \frac{\partial}{\partial x}\left(-\kappa(\xi)\frac{\partial T}{\partial x}\right) + \frac{\partial}{\partial y}\left(-\kappa(\xi)\frac{\partial T}{\partial y}\right) = 0. \tag{S9}$$

We also consider a wavelike temperature field modulated by the Bloch function of $F(\xi)$,

$$T = F(\xi)\mathrm{e}^{\mathrm{i}(\beta x - \omega t)} = \big(\textstyle\sum_s F_s \mathrm{e}^{\mathrm{i}sG\xi}\big)\mathrm{e}^{\mathrm{i}(\beta x - \omega t)}, \tag{S10}$$

with parameters of $s = 0, \pm1, \cdots, \pm\infty$ and $F_0 = 1$. Then, we can derive the partial derivative of temperature concerning time or space,

$$\frac{\partial T}{\partial t} = -\mathrm{i}\omega\big(\textstyle\sum_s F_s \mathrm{e}^{\mathrm{i}sG\xi}\big)\mathrm{e}^{\mathrm{i}(\beta x - \omega t)}, \tag{S11a}$$

$$\frac{\partial T}{\partial x} = \mathrm{i}\big(\textstyle\sum_s (\beta + sG)F_s \mathrm{e}^{\mathrm{i}sG\xi}\big)\mathrm{e}^{\mathrm{i}(\beta x - \omega t)}, \tag{S11b}$$

$$\frac{\partial T}{\partial y} = \mathrm{i}\big(\textstyle\sum_s sG\zeta F_s \mathrm{e}^{\mathrm{i}sG\xi}\big)\mathrm{e}^{\mathrm{i}(\beta x - \omega t)}. \tag{S11c}$$

We can also rewrite the spatially-periodic parameters described by Eqs. (S7a) and (S7b) with Fourier expansions,

$$\rho(\xi) = \textstyle\sum_{r=0,\pm1} \rho_r \mathrm{e}^{\mathrm{i}rG\xi}, \tag{S12a}$$

$$\kappa(\xi) = \textstyle\sum_{r=0,\pm1} \kappa_r \mathrm{e}^{\mathrm{i}rG\xi}, \tag{S12b}$$

with definitions of $\rho_{\pm1} = \mathrm{e}^{\pm\mathrm{i}\theta}\rho_0\Delta_\rho/2$ and $\kappa_{\pm1} = \kappa_0\Delta_\kappa/2$. We can further obtain

$$\rho(\xi)\frac{\partial T}{\partial t} = -\mathrm{i}\omega\left(\sum_s\sum_{r=0,\pm1}\rho_r F_{s-r}\mathrm{e}^{\mathrm{i}sG\xi}\right)\mathrm{e}^{\mathrm{i}(\beta x-\omega t)}, \tag{S13a}$$

$$\phi\rho_a u_y\frac{\partial T}{\partial y} = \mathrm{i}\phi\rho_a u_y\left(\sum_s sG\zeta F_s\mathrm{e}^{\mathrm{i}sG\xi}\right)\mathrm{e}^{\mathrm{i}(\beta x-\omega t)}, \tag{S13b}$$

$$-\kappa(\xi)\frac{\partial T}{\partial x} = -\mathrm{i}\left(\sum_s\sum_{r=0,\pm1}\kappa_r(\beta+(s-r)G)F_{s-r}\mathrm{e}^{\mathrm{i}sG\xi}\right)\mathrm{e}^{\mathrm{i}(\beta x-\omega t)}, \tag{S13c}$$

$$-\kappa(\xi)\frac{\partial T}{\partial y} = -\mathrm{i}\left(\sum_s\sum_{r=0,\pm1}\kappa_r(s-r)G\zeta F_{s-r}\mathrm{e}^{\mathrm{i}sG\xi}\right)\mathrm{e}^{\mathrm{i}(\beta x-\omega t)}. \tag{S13d}$$

We can further derive

$$\frac{\partial}{\partial x}\left(-\kappa(\xi)\frac{\partial T}{\partial x}\right) = \left(\sum_s(\beta+sG)\sum_{r=0,\pm1}\kappa_r(\beta+(s-r)G)F_{s-r}\mathrm{e}^{\mathrm{i}sG\xi}\right)\mathrm{e}^{\mathrm{i}(\beta x-\omega t)}, \tag{S14a}$$

$$\frac{\partial}{\partial y}\left(-\kappa(\xi)\frac{\partial T}{\partial y}\right) = \left(\sum_s sG\zeta\sum_{r=0,\pm1}\kappa_r(s-r)G\zeta F_{s-r}\mathrm{e}^{\mathrm{i}sG\xi}\right)\mathrm{e}^{\mathrm{i}(\beta x-\omega t)}. \tag{S14b}$$

Finally, we can express the component form of Eq. (S9) as

$$-\mathrm{i}\omega\left(\sum_{r=0,\pm1}\rho_r F_{s-r}\right) + \mathrm{i}\phi\rho_a u_y sG\zeta F_s$$

$$+(\beta+sG)\sum_{r=0,\pm1}\kappa_r(\beta+(s-r)G)F_{s-r} + sG\zeta\sum_{r=0,\pm1}\kappa_r(s-r)G\zeta F_{s-r} = 0. \tag{S15}$$

To derive the numerical results, we consider the parameters of $s = 0, \pm1, \cdots, \pm10$, and $F_{|s|>10} = 0$ in Eq. (S15), and then obtain twenty-one equations with twenty-one unknown numbers of β and $F_{|s|\leq10}$. Due to the assumption of $\mathrm{Re}[\beta] \ll G$, we do not need to linearly combine the solutions to β because the lattice effect is too weak to affect the intrinsic wavenumber of the wavelike temperature field. In other words, it is reasonable to choose the solution with the main effect and neglect the others. After obtaining the value of β, we can further calculate the propagating speed of wavelike temperature fields by $v = \omega/\mathrm{Re}[\beta]$ and derive the speed ratio of $\eta = |v_f/v_b| = |\mathrm{Re}[\beta_b]/\mathrm{Re}[\beta_f]|$.

Supplemental Note III: Critical point of $\Lambda = 1$

We have revealed that $\Lambda = \Delta_\rho\cos\theta/\Delta_\kappa = 1$ is the critical point for the transition between types I and II in the main text, which is also robust against different $\zeta = d/h$. Therefore, we

discuss in detail what happens at the critical point of $\Lambda = 1$ and focus on the dimensionless thermal diffusivity of $\overline{D}(\xi)$,

$$\overline{D}(\xi) = D(\xi)/D_0 = \frac{1+\Delta_\kappa \cos(G\xi)}{1+\Delta_\rho \cos(G\xi+\theta)}, \tag{S16}$$

with a definition of $D(\xi) = \kappa(\xi)/\rho(\xi)$. Since the vertical advection is applied, we focus on the effective dimensionless thermal diffusivity of $\overline{D}_e$ in the vertical direction, which can be calculated by the series connection,

$$\overline{D}_e = \frac{1}{\frac{1}{h}\int_0^h \frac{dy}{\overline{D}(\xi)}} = \frac{1}{\frac{1}{h}\int_0^h \frac{1+\Delta_\rho \cos(G\xi+\theta)}{1+\Delta_\kappa \cos(G\xi)} dy} = \frac{1}{1+(\Lambda-1)\left(1-\left(1-\Delta_\kappa^2\right)^{-1/2}\right)}. \tag{S17}$$

A feature of Eq. (S17) is that $\Lambda = 1$ always leads to $\overline{D}_e = 1$, indicating that the effective thermal diffusivity after spatial modulations is equal to the thermal diffusivity without spatial modulations. This feature provides a hint to explain the critical point of $\Lambda = 1$. Moreover, the $\overline{D}_e - \Lambda$ curves are also plotted in Fig. S2, which are overlapped except for the different domains induced by different values of Δ_ρ, so Λ is a meaningful parameter indeed.

Supplemental Note IV: Mechanism of diffusive Fizeau drag

We discuss the underlying mechanism based on the analytical results with two approximations. The first one is to consider $s = 0, \pm 1$ and $F_{|s|>1} = 0$ in Eq. (S15), and then we can derive three equations from Eq. (S15),

$$\begin{aligned} &-\mathrm{i}\omega(\rho_0 F_0 + \rho_{+1} F_{-1} + \rho_{-1} F_{+1}) \\ &+\beta(\kappa_0 \beta F_0 + \kappa_{+1}(\beta - G) F_{-1} + \kappa_{-1}(\beta + G) F_{+1}) = 0, \end{aligned} \tag{S18a}$$

$$\begin{aligned} &-\mathrm{i}\omega(\rho_0 F_{+1} + \rho_{+1} F_0) + \mathrm{i}\phi \rho_a u_y G\zeta F_{+1} \\ &+(\beta + G)(\kappa_0(\beta + G) F_{+1} + \kappa_{+1}\beta F_0) + G^2\zeta^2 \kappa_0 F_{+1} = 0, \end{aligned} \tag{S18b}$$

$$\begin{aligned} &-\mathrm{i}\omega(\rho_0 F_{-1} + \rho_{-1} F_0) - \mathrm{i}\phi \rho_a u_y G\zeta F_{-1} \\ &+(\beta - G)(\kappa_0(\beta - G) F_{-1} + \kappa_{-1}\beta F_0) + G^2\zeta^2 \kappa_0 F_{-1} = 0. \end{aligned} \tag{S18c}$$

Then, we consider the second approximation of $\mathrm{Re}[\beta] \ll G$, so Eqs. (S18a)-(S18c) can be further reduced to

$$-\mathrm{i}\omega(\rho_0 F_0 + \rho_{+1}F_{-1} + \rho_{-1}F_{+1}) + \beta(\kappa_0\beta F_0 - \kappa_{+1}GF_{-1} + \kappa_{-1}GF_{+1}) = 0, \quad \text{(S19a)}$$

$$-\mathrm{i}\omega(\rho_0 F_{+1} + \rho_{+1}F_0) + \mathrm{i}\phi\rho_a u_y G\zeta F_{+1}$$

$$+G(\kappa_0 GF_{+1} + \kappa_{+1}\beta F_0) + G^2\zeta^2\kappa_0 F_{+1} = 0, \quad \text{(S19b)}$$

$$-\mathrm{i}\omega(\rho_0 F_{-1} + \rho_{-1}F_0) - \mathrm{i}\phi\rho_a u_y G\zeta F_{-1}$$

$$+G(\kappa_0 GF_{-1} - \kappa_{-1}\beta F_0) + G^2\zeta^2\kappa_0 F_{-1} = 0. \quad \text{(S19c)}$$

The solutions to Eqs. (S19b) and (S19c) can be expressed as

$$F_{+1} = \frac{-G\beta\kappa_{+1} + \mathrm{i}\omega\rho_{+1}}{G^2(1+\zeta^2)\kappa_0 + \mathrm{i}G\zeta\phi\rho_a u_y}, \quad \text{(S20a)}$$

$$F_{-1} = \frac{G\beta\kappa_{-1} + \mathrm{i}\omega\rho_{-1}}{G^2(1+\zeta^2)\kappa_0 - \mathrm{i}G\zeta\phi\rho_a u_y}. \quad \text{(S20b)}$$

The substitution of Eqs. (S20a) and (S20b) into Eq. (S19a) yields

$$-\mathrm{i}\omega\rho_0 + \beta^2\kappa_0\left(1 - \frac{\Delta_\kappa^2}{2((1+\zeta^2)^2+\zeta^2\Gamma^2)}\right)$$

$$+\omega^2\frac{(1+\zeta^2)\kappa_0}{\phi^2\epsilon^2 u_y^2}\frac{\Delta_\rho^2\Gamma^2}{2((1+\zeta^2)^2+\zeta^2\Gamma^2)} + \beta\omega\frac{\zeta\kappa_0}{\phi\epsilon u_y}\frac{\Delta_\rho\Delta_\kappa\Gamma^2\cos\theta}{(1+\zeta^2)^2+\zeta^2\Gamma^2} = 0, \quad \text{(S21)}$$

with definitions of $\Gamma = \phi\epsilon u_y/(GD_0)$, $\epsilon = \rho_a/\rho_0$, and $D_0 = \kappa_0/\rho_0$.

We further consider $T_0 = \mathrm{e}^{\mathrm{i}(\beta x - \omega t)}$, $\partial_t = -\mathrm{i}\omega$, and $\partial_x = \mathrm{i}\beta$, so Eq. (S21) can be rewritten as

$$\rho_0\frac{\partial T_0}{\partial t} - \kappa_e\frac{\partial^2 T_0}{\partial x^2} - \sigma_1\frac{\partial^2 T_0}{\partial t^2} + \sigma_2\frac{\partial^2 T_0}{\partial t\partial x} = 0, \quad \text{(S22)}$$

with the homogenized parameters expressed as

$$\kappa_e = \kappa_0\left(1 - \frac{\Delta_\kappa^2}{2((1+\zeta^2)^2+\zeta^2\Gamma^2)}\right), \quad \text{(S23a)}$$

$$\sigma_1 = \frac{(1+\zeta^2)\kappa_0}{\phi^2\epsilon^2 u_y^2}\frac{\Delta_\rho^2\Gamma^2}{2((1+\zeta^2)^2+\zeta^2\Gamma^2)}, \quad \text{(S23b)}$$

$$\sigma_2 = \frac{\zeta\kappa_0}{\phi\epsilon u_y}\frac{\Delta_\rho\Delta_\kappa\Gamma^2\cos\theta}{(1+\zeta^2)^2+\zeta^2\Gamma^2}. \quad \text{(S23c)}$$

The homogenized equation [i.e., Eq. (S22)] does not contain any horizontal synthetic

advection related to the term of ∂_x, so the vertical advection does not affect the horizontal heat transfer directly. Surprisingly, there are two additional high-order terms of ∂_t^2 and $\partial_t \partial_x$ in Eq. (S22). As described by the Fourier law, the constitutive relation should be $J = -\kappa_e \partial_x T_0$, where J is the horizontal heat flux. Considering the energy conservation of heat transfer, we can derive $\rho_0 \partial_t T_0 + \partial_x J = 0$, which further yields $\rho_0 \partial_t T_0 - \kappa_e \partial_x^2 T_0 = 0$. However, this is not the case described by Eq. (S22), so the constitutive relation described by the Fourier law should be modified after homogenization. According to Eq. (S22), we can rewrite the constitutive relation as

$$\tau \frac{\partial J}{\partial t} + J = -\kappa_e \frac{\partial T_0}{\partial x} + \sigma_2 \frac{\partial T_0}{\partial t}. \tag{S24}$$

The term of $\tau \partial_t J$ has a mathematical correspondence to thermal relaxation [1-3] with the relaxation time of $\tau = -\sigma_1/\rho_0$. The term of $-\kappa_e \partial_x T_0$ reflects the conductive contribution related to the temperature gradient. Unusually, the term of $\sigma_2 \partial_t T_0$ demonstrates that the horizontal heat flux is coupled with the temperature change rate. Similar to acoustic Willis coupling between stress and velocity or between momentum and strain, we can attribute the modified constitutive relation described by Eq. (S24) to thermal Willis coupling between heat flux and temperature change rate. Naturally, $\sigma_2 \partial_t T_0$ can be referred to as the thermal Willis term and σ_2 is the thermal Willis coefficient. Thermal Willis coupling uniquely occurs in an inhomogeneous medium because the horizontal heat flux cannot be coupled with the temperature change rate in a homogeneous medium. Specifically, a macroscopically homogeneous medium with the parameter of $d = 0$ leads to $\sigma_2 = 0$, so thermal Willis coupling disappears. Moreover, the vertical advection is also indispensable for thermal Willis coupling because $u_y = 0$ also yields $\sigma_2 = 0$, indicating the vanish of thermal Willis coupling.

Nevertheless, since Eq. (S22) is obtained from two approximations of $s = 0, \pm 1$ and $\mathrm{Re}[\beta] \ll G$, the modified constitutive relation described by Eq. (S24) is also approximate, but it can still provide a qualitative explanation on diffusive Fizeau drag.

To look into the speed difference generated by thermal Willis coupling, we further perform analytical calculations based on Eq. (S22),

$$-\mathrm{i}\omega\rho_0 + \beta^2\kappa_e + \omega^2\sigma_1 + \beta\omega\sigma_2 = 0. \tag{S25}$$

We also suppose $\beta = p + \mathrm{i}q$, and Eq. (S25) can be rewritten as

$$-\mathrm{i}\omega\rho_0 + (p + \mathrm{i}q)^2\kappa_e + \omega^2\sigma_1 + (p + \mathrm{i}q)\omega\sigma_2 = 0, \tag{S26}$$

which can be further decomposed into

$$(p^2 - q^2)\kappa_e + \omega^2\sigma_1 + p\omega\sigma_2 = 0, \tag{S27a}$$

$$-\omega\rho_0 + 2pq\kappa_e + q\omega\sigma_2 = 0. \tag{S27b}$$

The solutions to Eqs. (S27a) and (S27b) can be written as

$$p_{f,b} = \frac{-2\omega\sigma_2 \pm \sqrt{2}\gamma}{4\kappa_e}, \tag{S28a}$$

$$q_{f,b} = \pm\frac{\sqrt{2}\gamma\left(8\omega^2\kappa_e\sigma_1 - 2\omega^2\sigma_2^2 + \gamma^2\right)}{16\omega\rho_0\kappa_e^2}, \tag{S28b}$$

with a definition of $\gamma = \sqrt{\omega^2(-4\kappa_e\sigma_1 + \sigma_2^2) + \sqrt{\omega^4(-4\kappa_e\sigma_1 + \sigma_2^2)^2 + 16\omega^2\rho_0^2\kappa_e^2}}$. Since $|p_f|$ and $|p_b|$ are two different numbers, we can observe a speed difference of temperature field propagation in two opposite directions. In contrast, q_f and q_b are always two opposite numbers, indicating the same spatial decay rates in two opposite directions.

We can also calculate the wavenumber difference of $\Delta\mathrm{Re}[\beta]$ by

$$\Delta\mathrm{Re}[\beta] = p_f + p_b = -\sigma_2\omega/\kappa_e. \tag{S29}$$

$\Delta\mathrm{Re}[\beta]$ is in direct proportion to ω, which is in qualitative agreement with the numerical results shown in Fig. 3(b) in the main text. Meanwhile, $\Delta\mathrm{Re}[\beta]$ is crucially determined by the

thermal Willis coefficient of σ_2. Since both $u_y = 0$ and $u_y = \infty$ lead to $\sigma_2 = 0$, thermal Willis coupling vanishes accordingly. As a result, the wavenumber difference (or the speed difference) also disappears when $2\pi\Gamma = 0$ and $2\pi\Gamma = \infty$, which agrees well with the numerical results shown in Fig. 2 in the main text. Therefore, the wavenumber difference (or the speed difference) mainly depends on thermal Willis coupling described by the term of $\sigma_2 \partial_t T_0$.

Comparing Eqs. (S5a) and (S5b) and Eqs. (S28a) and (S28b), we can draw the following conclusion. The horizontal advection cannot contribute to a speed difference but can lead to different spatial decay rates of temperature field propagation in two opposite directions. On the contrary, thermal Willis coupling can yield a speed difference but cannot generate different spatial decay rates of temperature field propagation in two opposite directions. Nevertheless, since the results described by Eqs. (S28a) and (S28b) are obtained from two approximations, slightly different spatial decay rates in two opposite directions can still be observed.

Supplemental Note V: Another approach to generating wavelike temperature fields

We can also generate a wavelike temperature field by setting an initial temperature of $T(t = 0) = \mathrm{e}^{\mathrm{i}\beta x}$, thereby resulting in a real β and a complex ω. The imaginary part of ω reflects the temporal decay rate of wavelike temperature fields. To some extent, this approach has a duality to the case discussed in the main text, i.e., applying a periodic source with a temperature of $T(x = 0) = \mathrm{e}^{-\mathrm{i}\omega t}$. The method to derive the numerical solution to ω is to take ω as an unknown number instead of β in Eq. (S15). A nonzero $\mathrm{Re}[\omega]$ indicates the horizontal symmetry breaking because a wavelike temperature field propagates along a specific direction, i.e., forward with $\mathrm{Re}[\omega] > 0$ and backward with $\mathrm{Re}[\omega] < 0$.

Then we discuss the real part of ω, which further determines the propagating speed of wavelike temperature fields by $v = \mathrm{Re}[\omega]/\beta$ (the solid curves in Fig. S3). For comparison, we also plot the speed ratio of $\eta = \left|\mathrm{Re}[\beta_b]/\mathrm{Re}[\beta_f]\right|$ with dotted curves in Fig. S3. The parameters for the two approaches are the same. The only difference is that we take ω as an unknown number and β as a known number when calculating v, but take β as an unknown number and ω as a known number when calculating η. The $v - 2\pi\Gamma$ curves and $\eta - 2\pi\Gamma$ curves in Fig. S3 have a mirror symmetry in the horizontal direction.

Similar to the three types of $\eta - 2\pi\Gamma$ curves presented in Figs. 2(b)-2(d) in the main text, we also find three types of $v - 2\pi\Gamma$ curves in Fig. S3(a). The first one features that v is always smaller than 0 (the bottom three solid curves). The second one features that v is first smaller and then larger than 0 (the fourth and fifth solid curves from the bottom). The third one features that v is always larger than 0 (the top solid curve). Since $\theta = \pi/2$ always leads to $\Lambda = 0$, the solid (or dotted) curves in Fig. S3(b) are irrelevant to Δ_ρ. We further take the solid and dotted curves with the parameter of $\Lambda = 0$ in Fig. S3(a) as an example to demonstrate the unique property of thermal Willis coupling. Due to $v > 0$, a wavelike temperature field propagates forward, so we may conceive that there is a forward drive in the system. However, $\eta < 1$ means that the forward speed is slower than the backward one. Generally, if there is a forward drive in the system, the forward speed should be faster than the backward one. Comparing the other solid and dotted curves with the same parameter of Λ in Fig. S3(a) or with the same parameter of Δ_ρ in Fig. S3(b), we can draw the following conclusion. If we preset a real wavenumber by constructing an initial wavelike temperature profile, the temperature field propagates forward (or backward). If we preset a real angular

frequency by applying a periodic temperature source, the forward speed is, however, slower (or faster) than the backward one. This contradiction demonstrates the intriguing behavior of thermal Willis coupling. Since thermal Willis coupling is related to the coupling between heat flux and temperature change rate, it is crucially dependent on the initial and boundary conditions. Therefore, when we use two different approaches to generate wavelike temperature fields, the corresponding results might also be different.

References

[1] D. D. Joseph and L. Preziosi, Heat waves, Rev. Mod. Phys. **61**, 41 (1989).

[2] B.-D. Nie and B.-Y. Cao, Three mathematical representations and an improved ADI method for hyperbolic heat conduction, Int. J. Heat Mass Transf. **135**, 974 (2019).

[3] M. Gandolfi, G. Benetti, C. Glorieux, C. Giannetti, and F. Banfi, Accessing temperature waves: A dispersion relation perspective, Int. J. Heat Mass Transf. **143**, 118553 (2019).

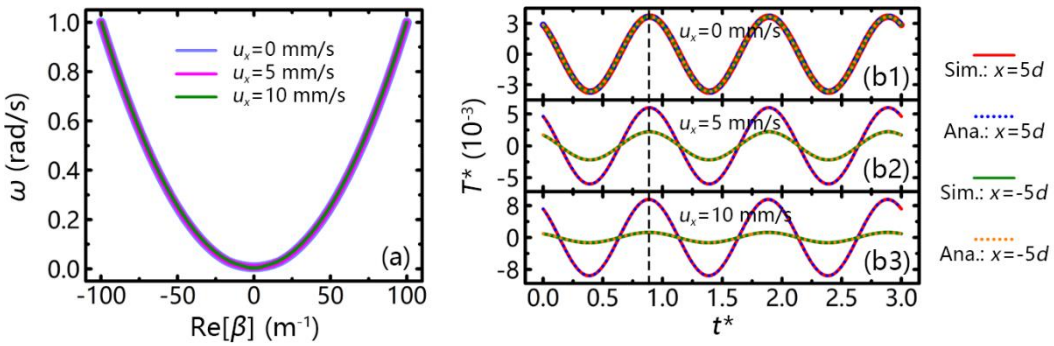

Fig. S1. Features of conventional heat transfer. (a) Thermal dispersion. (b1)-(b3) Evolution of T^* with different horizontal advection speeds. The vertical dashed line marks the temperature peaks. The system has translational symmetry in the vertical direction. Parameters: $\phi = 0.1$, $\epsilon = 1$, $D_0 = 5 \times 10^{-5}$ m^2/s, $d = 0.02$ m, $h = 0.02$ m, and $t_0 = 20$ s. The simulation length is $30d = 0.6$ m. The left and right boundaries are insulated. The upper and lower boundaries are set with periodic conditions. Sim.: Simulation; and Ana.: Analytical.

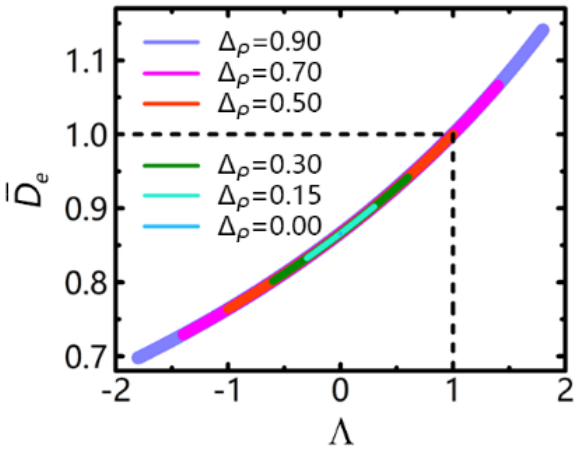

Fig. S2. Effective dimensionless thermal diffusivity of $\bar{D}_e$ in the vertical direction as a function of $\Lambda = \Delta_\rho \cos\theta / \Delta_\kappa$. Λ is tuned by θ. Parameters: $\Delta_\kappa = 0.5$, $d = 0.02$ m, and $h = 0.02$ m.

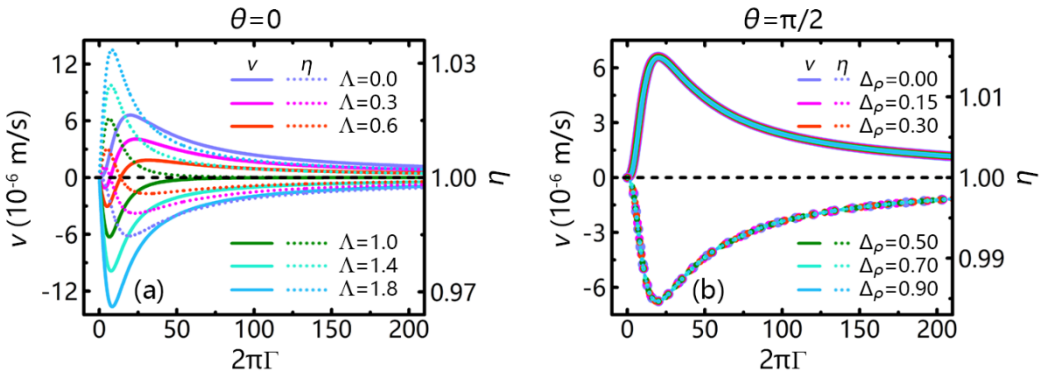

Fig. S3. Comparison between two approaches. Velocity of v (solid curves corresponding to the left axis) and speed ratio of η (dotted curves corresponding to the right axis) as a function of $2\pi\Gamma = \phi\epsilon u_y d/D_0$ when (a) $\theta = 0$ or (b) $\theta = \pi/2$. Except the parameters presented in (a) and (b), the others are $\phi = 0.1$, $\epsilon = 1$, $D_0 = 5 \times 10^{-5}$ m^2/s, $\Delta_\kappa = 0.5$, $d = 0.02$ m, and $h = 0.02$ m. When we calculate $v = \mathrm{Re}[\omega]/\beta$, β is a known number equal to 10π m^{-1}. When we calculate $\eta = \left|\mathrm{Re}[\beta_b]/\mathrm{Re}[\beta_f]\right|$, ω is a known number equal to $\pi/10$ rad/s.